iJRASET
International Journal For Research in Applied Science and Engineering Technology

INTERNATIONAL JOURNAL FOR RESEARCH

IN APPLIED SCIENCE & ENGINEERING TECHNOLOGY

Volume: 10 **Issue:** I **Month of publication:** January 2022

DOI: https://doi.org/10.22214/ijraset.2022.40035

www.ijraset.com

Call: 08813907089 | E-mail ID: ijraset@gmail.com

International Journal for Research in Applied Science & Engineering Technology (IJRASET)
ISSN: 2321-9653; IC Value: 45.98; SJ Impact Factor: 7.538
Volume 10 Issue I Jan 2022- Available at www.ijraset.com

Performance Performance Analysis of Tubular PEM Fuel Cell Models and Thermal Analysis of Base Model using Ethylene Glycol-Water Mixture as a Coolant

Tejas Ambekar[1], Prathmesh Amle[2], Durgesh Chandangole[3], Gopal Ghule[4], Prof. Dr. L. D. Mangate[5]
[1, 2, 3, 4]*Students, Mechanical Engineering, Vishwakarma Institute of Technology, Pune, India*
[5]*Faculty, Mechanical Engineering, Vishwakarma Institute of Technology, Pune, India*

Abstract: ***This work aims towards the simulation of Various proton exchange membrane fuel cell (PEMFC) models to investigate the effects of operating parameters such as temperature, pressure, anode flow levels and cathode reactants, component types, cooling temperatures in the performance of a modified fuel cell. The basic model and the tubular model are developed in modelling software based on the size of the parameter later simulated using the addon module in the Ansys software. The Addon module is specifically designed to mimic a different type of fuel cell. The simulated model of cell power output showed positive compliance with experimental results taken from the literature and revealed that the operating pressure, temperature, and flow rate of reactants positively affect the function of the Fuel cell. The results also showed that the cooling temperature of the coolant indicates higher concentrations of current congestion compared to the base model without cooling. Corrective results obtained from the effect of temperature on cell function showed that the fuel cell temperature favor both cell function and efficiency. It can therefore be assumed that the efficiency of the cell is strongly influenced by operating temperature, pressure, cooling temperature, fuel flow rate and oxidant.***
Keywords: PEM fuel cell, Current density, tubular fuel cell, addon-module.

I. INTRODUCTION

Over the years, the earth has relied heavily on the only source of energy known as fossil fuels and is limited to domestic and industrial use. This situation has created an imbalance in global oil production and demand, which has led to energy crisis due to a lack of supply and price volatility. Inflation and environmental pollution of fossil fuels are some of the major problems caused by over-reliance on this energy source. It has been widely documented that the burning of fossil fuels poses a threat to human health and the environment and that this has led to an increase in the search for a clean energy source to protect the environment and to protect one from inhaling toxic substances. For example, it is a well-known fact that combustion of fossil fuels emits harmful gases such as CO2, CO, and SO2 into the atmosphere. These gases pose a serious health and environmental risk and, therefore, create a major global environmental problem. Concerns about price volatility due to over-reliance on fossil fuels and increased awareness of the natural impact of fossil fuel fuels have led to an increase in calls for other energy sources that may not compete effectively with existing energy sources. Fuel cells defined as electrochemical tools that convert chemical reaction energy into electricity directly, with water as their product, are now considered a promising, economical, and sustainable energy source.

Fuel cells produce little or no pollution depending on the type of fuel used. They also have advantages that make them better than other industrial combustion channels which are capable of capturing the excess heat produced and using it in the same way as mixing or heating space / water. Other major advantages of fuel cells carried over combustible engines include high efficiency and lack of exhaust hazardous substances. Unless researchers and the government provide the recognition of fuel cells especially the proton exchange membrane fuel cell (PEMFC) as a non-environmentally friendly source of energy that can compete effectively with existing energy sources, the high cost of associated components and technological management is detrimental. commercial commercial availability of fuel cells as an alternative energy source. Over the past few years, good progress has been made in achieving the sale of this unique energy source by reducing the cost of electrode components, flow field plate, and membranes. However, the lack of understanding of the impact of various parameters on the power output by the fuel cell system remains a critical issue to focus on in the current study.

ISSN: 2321-9653; IC Value: 45.98; SJ Impact Factor: 7.538
Volume 10 Issue I Jan 2022- Available at www.ijraset.com

In this note, the first and second rules of thermodynamics have been recognized as major tools for measuring the strength and power of fuel cell technology. The first law of thermodynamics (energy analysis) deals with the value of energy and states that energy cannot be created or destroyed. The law serves as a necessary tool for calculating power during the process and does not present challenges to the engineers. The second law (energy analysis), however, deals with energy quality, the deterioration of this energy during the process, the generation of entropy, and the loss of productivity and provides a large area for development. The second law of thermodynamics has been proven to be a powerful tool in the efficient operation of complex thermodynamic systems. In more recent times, energy analysis has become an important component in providing a better understanding of energy system processes analysis, inefficiency sources, and the differential quality of energy (or heat) used.

The purpose of this study is therefore to develop a predictable simul model to determine how we can increase fuel cell performance especially by using a coolant such as an ethyl glycol water compound and how we can increase the current energy produced by fuel cell function parameters. Imitation of the improved model is expected to provide information on the interaction of various parameters affecting the functioning of the proton exchange membrane fuel cell.

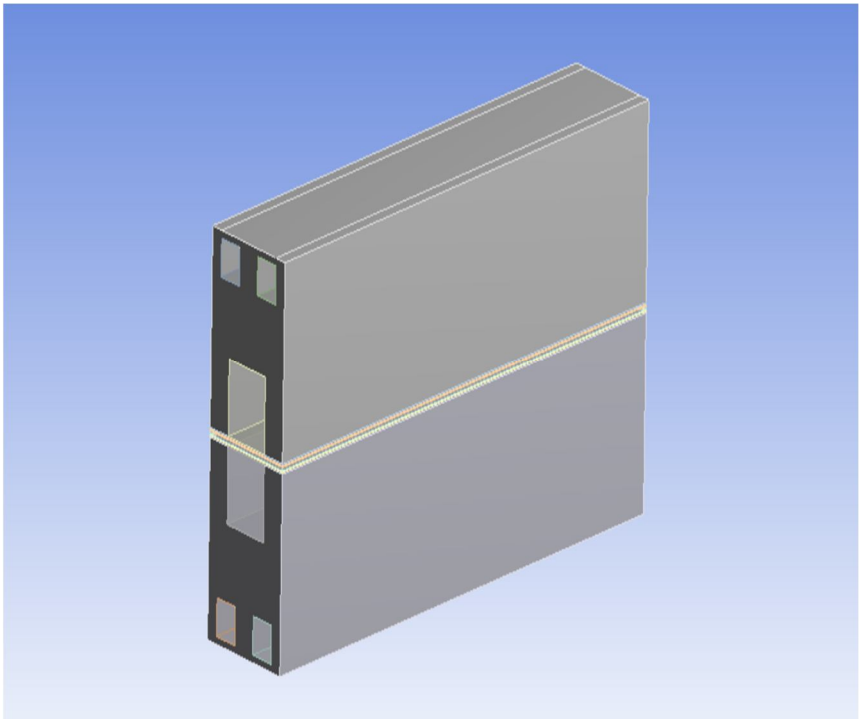

Fig.1 Base model

II. LITERATURE SURVEY

[1] A calorimeter was used to measure the heat production in (PEM) fuel cells operated on hydrogen and oxygen at 50 ◦C and 1 bar. We thus conclude that the reversible heat of the anode and cathode of this cell are near 0 and −80 J K−1 mol−1, respectively.[2] The salient numerical features of the models are examined, and an overview of the most used computational fluid dynamic codes for the numerical modelling of proton exchange membrane fuel cells is given. [3] A three-dimensional, multi-phase, non-isothermal CFD model of a proton exchange membrane fuel cell has been developed and used to investigate the displacement, deformation, and stresses inside the whole cell, which developed during the cell operation due to the changes of temperature. [4] Increasing the width of the channels reduces the maximum temperature of the cooling plate surface. Increasing the distance between two channels leads to adverse effects on the thermal parameters as well as increased pressure drop. [5] The effects of different parameters on the performances of proton exchange membrane fuel cells were studied experimentally. [6] Full three-dimensional computational fluid dynamics models of planar and tubular-shaped air-breathing PEM fuel cell has been developed.

The purpose of this study is therefore to develop a predictable simulation model to determine how we can increase fuel cell performance especially by using a coolant such as an ethyl glycol water compound and how we can increase the current energy produced by fuel cell function parameters. Imitation of the improved model is expected to provide information on the interaction of various parameters affecting the functioning of the proton exchange membrane fuel cell.

ISSN: 2321-9653; IC Value: 45.98; SJ Impact Factor: 7.538
Volume 10 Issue I Jan 2022- Available at www.ijraset.com

III.GEOMETRY DEFINITION

Due to the fact that there are a number of different physical zones associated with the fuel cell, the following regions must be present in the fuel cell mesh:

1) Anode flow channel
2) Anode gas diffusion layer
3) Anode catalyst layer
4) Membrane layer
5) Cathode catalyst layer
6) Cathode gas diffusion layer
7) Cathode flow channel
8) The following zones have to be identified, if present in the fuel cell mesh:
9) Anode current collector
10) Cathode current collector
11) Coolant channel

We have selected Maruti Suzuki Ertiga for drive shaft calculations. The following are the specifications of it.

TABLE I.
GEOMETRY DEFINATION FOR FUEL CELL AND ELECTROLYSIS MODEL

Cell dimension	Values (in mm)
Gas channel length	10
Height of gas channel	1
Width of gas channel	1
Width of cell	2
Thickness of catalyst layer	0.014
Thickness of gas diffusion layer	0.0254
Thickness of current collector	2.5
Thickness of membrane	0.051
Overall cell height	5.1295
Cooling channel width	0.5
Cooling channel height	0.5

TABLE II.
OPERATING CONDITIONS FOR FUEL CELL

Parameters	Value
Cell operating temperature	323 K
Cell operating pressure	1 bar
Open-circuit voltage	1.07 V
Anode Reference exchange current density	10000 A/m^2
Cathode Reference exchange current density	20 A/m^2
CL Electric conductivity	5000 S/m
Current collector Electric conductivity	1000000 S/m
GDL Electric conductivity	5000 S/m
Anode exchange coefficient	2
Cathode exchange coefficient	2
Reference concentration of anode	1 $kmol/m^3$
Reference concentration of cathode	1 $kmol/m^3$
CL Porosity	0.2
GDL Porosity	0.6

IV. SETUP

A. *Boundary condition*

TABLE III
BOUNDRY CONDITION

Location	Parameter	values
Cathode	Velocity inlet	0.3 m/s
	O2 mass fraction	0.6
	H2O mass fraction	0.4
	Pressure outlet	0 pa
	temperature inlet	353
Anode	Velocity inlet	0.2 m/s
	O2 mass fraction	0.21
	H2O mass fraction	0.15
	Pressure outlet	0 pa
	temperature inlet	353
Wall	Cathode Collector	0.2-0.64

B. *Mesh Quality Parameter*

TABLE IIV
MESH QAULITY PARAMETER

Quality Parameter	Max.		Min.		Avg.	
Aspects Ratio	Base model FC	11.905	Base model FC	1	Base model FC	2.0058
	Base model FC with cooling	11.905	Base model FC with cooling	1	Base model FC with cooling	2.0166
	Circular tubular FC	36.283	Circular tubular FC	1.06	Circular tubular FC	4.9456
	Square tubular FC	36.364	Square tubular FC	1.008	Square tubular FC	6.0151
	Triangular Tubular FC	111.31	Triangular Tubular FC	1.079	Triangular Tubular FC	6.4955
Element Quality	Base model FC	1	Base model FC	0.154	Base model FC	0.89663
	Base model FC with cooling	1	Base model FC with cooling	0.154	Base model FC with cooling	0.89076
	Circular tubular FC	0.9973	Circular tubular FC	0.05	Circular tubular FC	0.67422
	Square tubular FC	1	Square tubular FC	0.05	Square tubular FC	0.74809
	Triangular Tubular FC	0.9972	Triangular Tubular FC	0.05	Triangular Tubular FC	0.66669
Skewness	Base model FC	0.00	Base model FC	0.05	Base model FC	0.00

	Base model FC with cooling	0.4659	Base model FC with cooling	0.05	Base model FC with cooling	0.00
	Circular tubular FC	0.8685	Circular tubular FC	0.05	Circular tubular FC	0.16208
	Square tubular FC	0.9008	Square tubular FC	0.05	Square tubular FC	0.16789
	Triangular Tubular FC	0.9872	Triangular Tubular FC	0.05	Triangular Tubular FC	0.35204

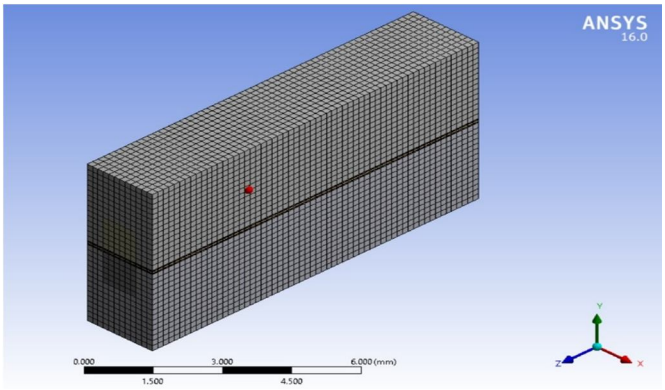

Fig. 2. Meshing of Base model

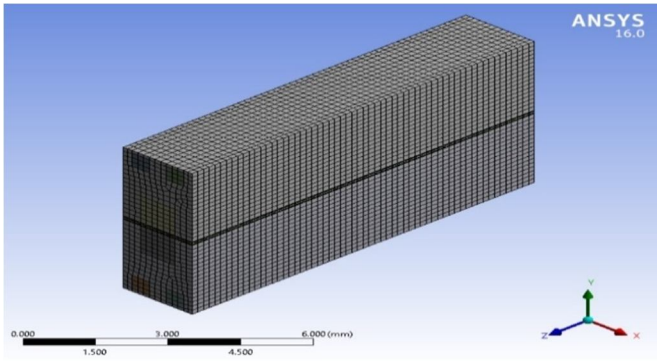

Fig. 3. Meshing of base model with cooling

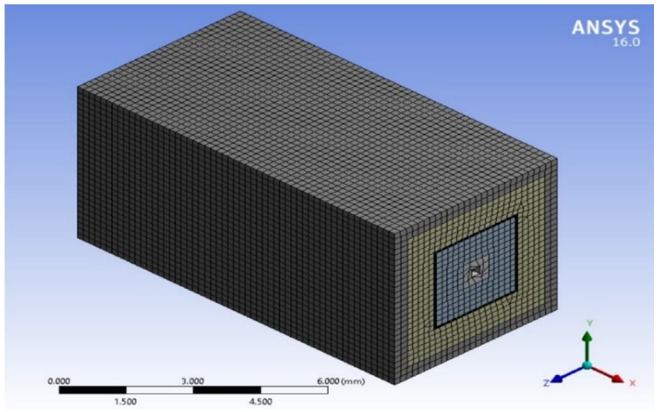

Fig. 4. Meshing of tubular square model

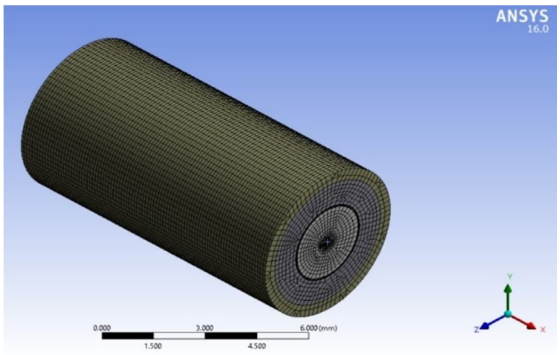

Fig. 5. Meshing of tubular circular model

C. Grid Independence Test

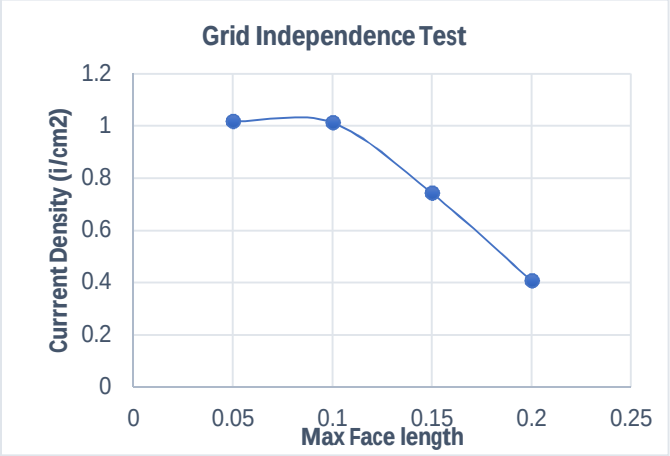

Fig. 6. Grid Independence Test

In this section, the resolution of the computational grid is evaluated. The appropriate number of grid points has a great impact on the accuracy of the numerical simulations. In order to test the effect of the number of grid points on numerical results, various grid resolutions are considered. The results are shown in Figure 3 in which the pressure drop is compared between the input and output of the fuel cell. The results show that the number of 25200 grid points is enough for the present simulation.

V. PROPERTIES OF ETHYL-GLYCOL MIXTURE

Ethylene glycol-water properties are observed at different temperatures and at different fraction. Properties observed are Thermal conductivity, density, viscosity, specific heat, electrical conductivity.

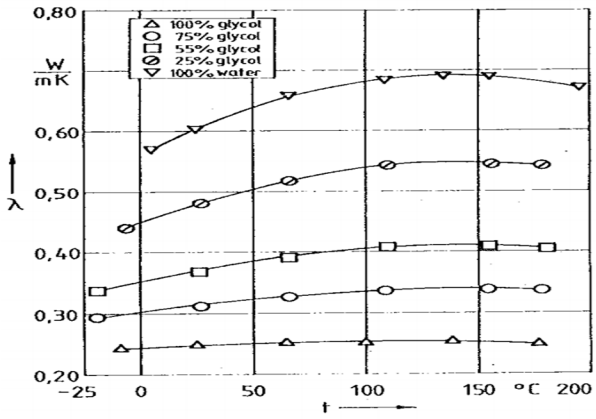

Fig. 7. Thermal conductivity of ethylene glycol-water mixtures

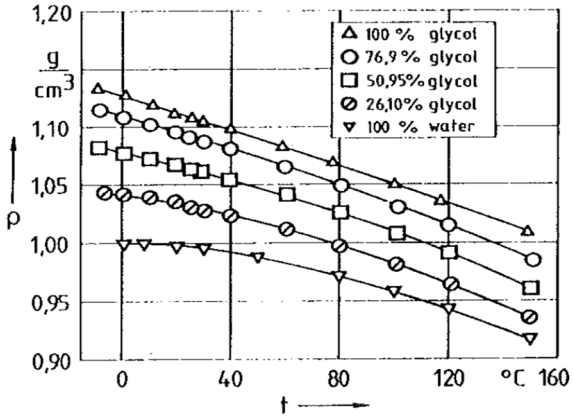

Fig. 8. Density of ethylene glycol-water mixture

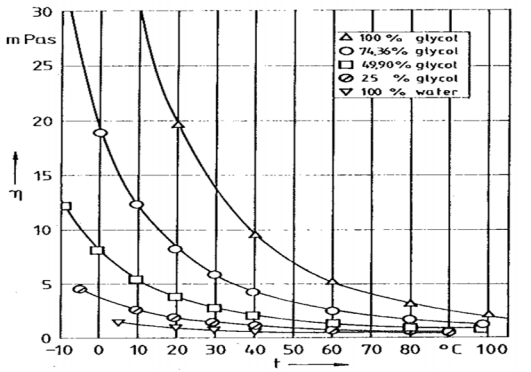

Fig. 9. Viscosity of ethylene glycol-water mixtures

VI. RESULTS AND DISCUSSION

A. Result for FC Base Model without Cooling

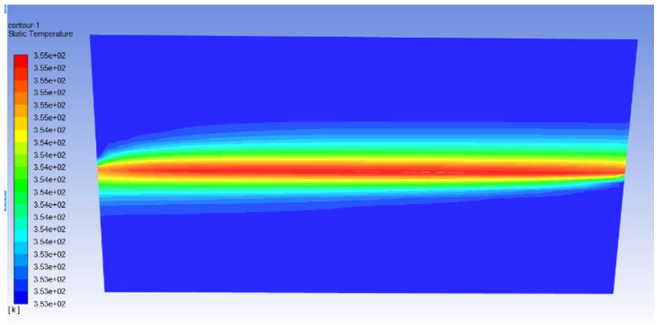

Fig. 10. Temperature distribution along the length of fuel cell

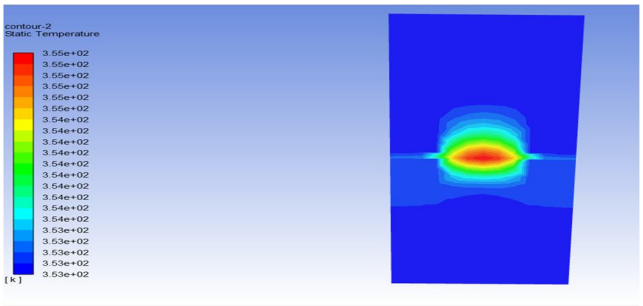

Fig. 11. Temperature distribution along the cross section of fuel cell

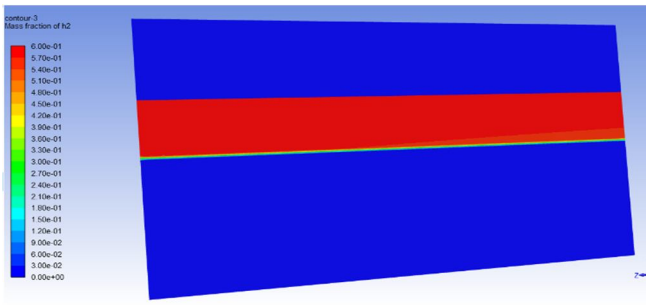

Fig. 12. H2 species fraction distribution along length of fuel cell

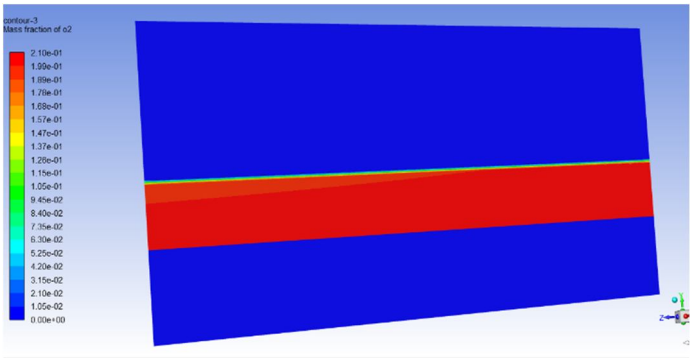

Fig. 13. O2 species fraction distribution along length of fuel cell

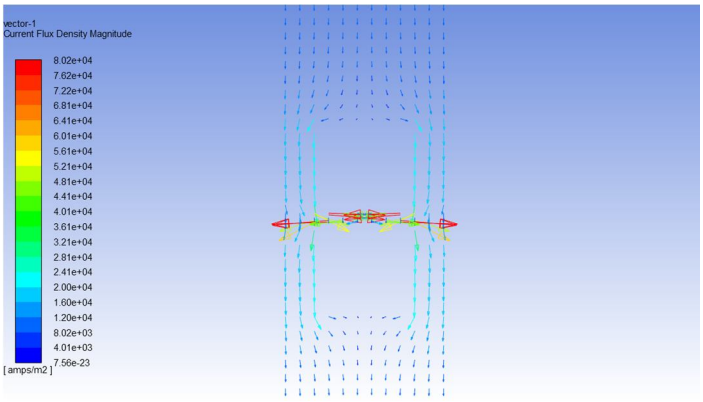

Fig. 14. Vector showing Current density magnitude within cross section of fuel cell

B. Identify Results for FC base model with cooling (Ethylene glycol-water 50:50).

Solution has monitor for current flux density and maximum temperature in fuel cell. It can be seen that solution is converged above 2500 iterations in case of non-cooling system of fuel cell.

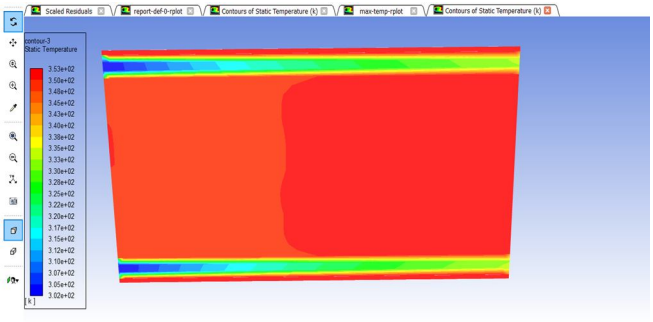

Fig. 15. Temperature distribution along the length of fuel cell

Distribution of heat at anode and cathode side are different. Cathode reaction generated more fraction out of total heat. Temperature distribution along the height of the fuel cell has been plotted in figure.

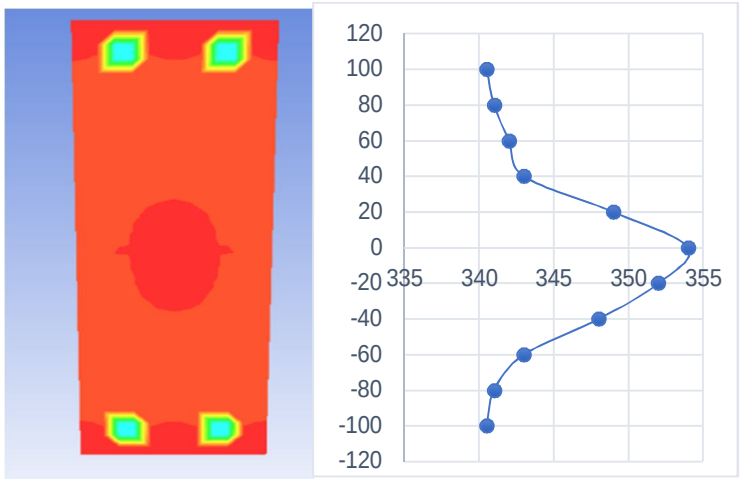

Fig. 16. Temperature distribution along the length of fuel cell

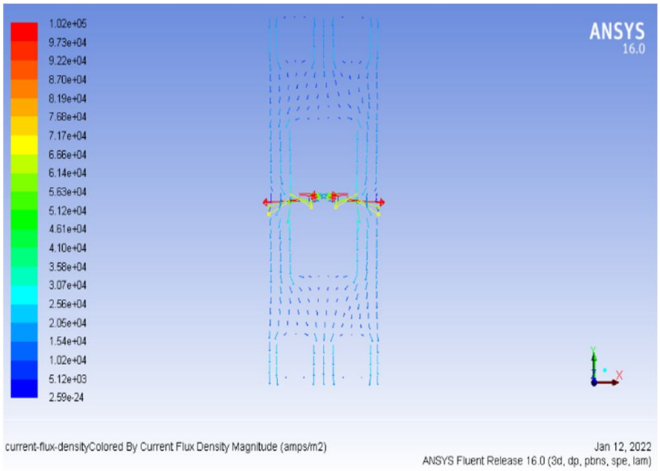

Fig. 17. Vector showing Current density magnitude within cross section of fuel cell

C. Results for Tubular circular FC Base Model

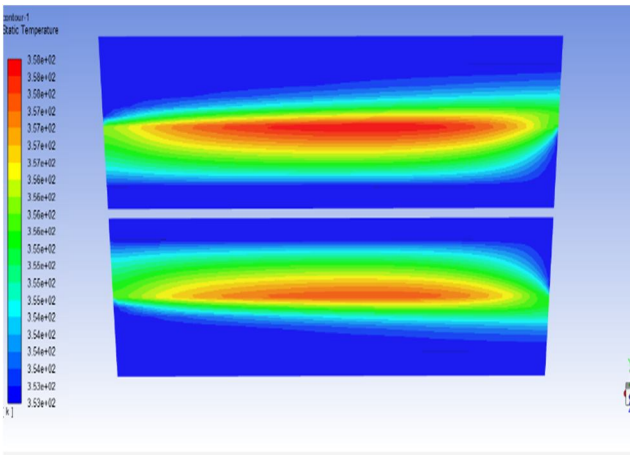

Fig. 18. Temperature distribution along the length of circular fuel cell

D. Results for Tubular square FC Base Model

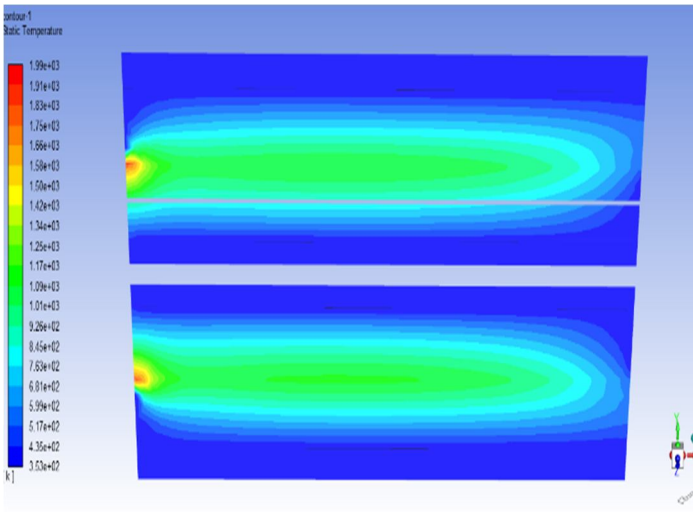

Fig. 19. Temperature distribution along the length of square c/s fuel cell

E. Graphs

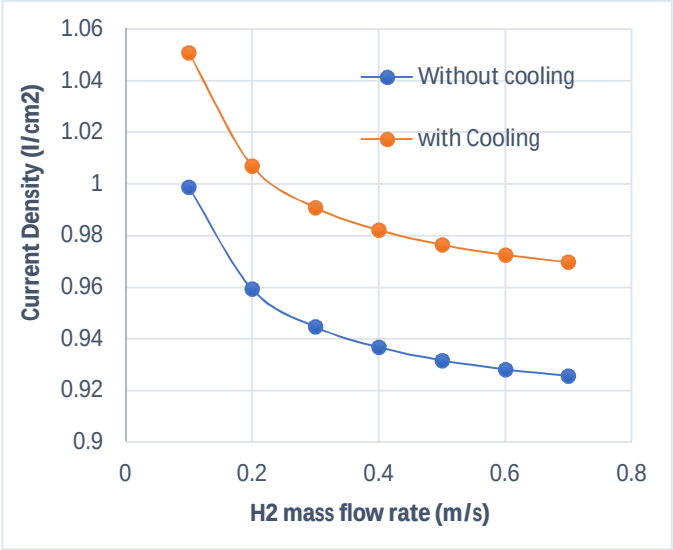

Fig. 20. Effect of H2 specie mass flow rate variation on current density

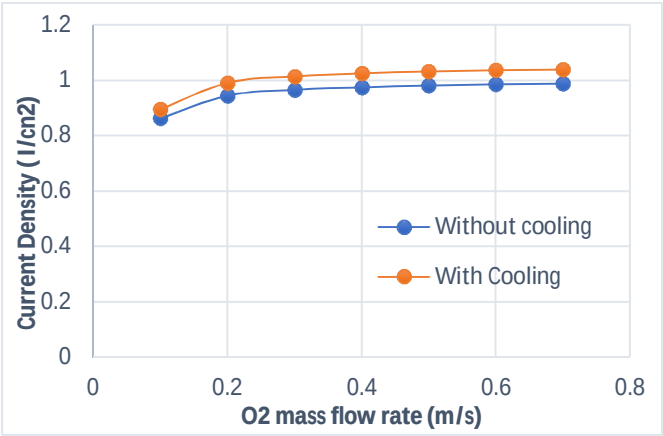

Fig. 21. Effect of H2 species and o2 species mass flow rate variation on current density

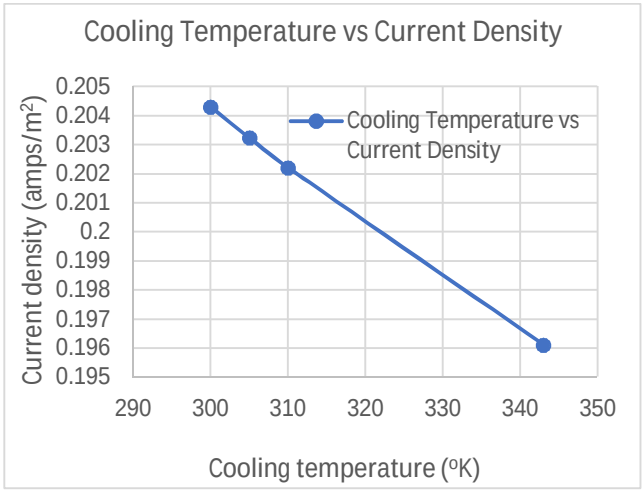

Fig. 22. Effect of cooling temperature variation on current density

F. Graphs With Respect to Tubular Circular Model

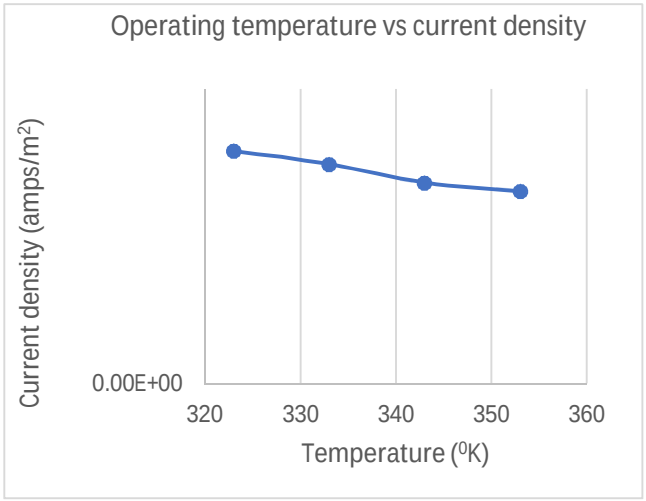

Fig. 23. Effect of temperature variation on current density in tubular circular FC

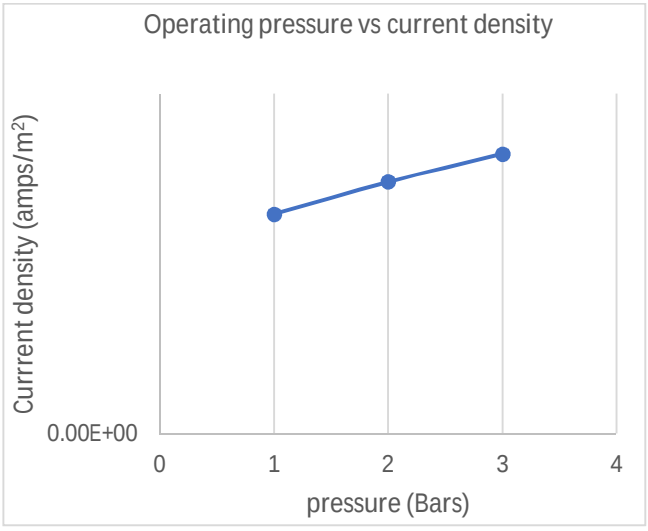

Fig. 24. Effect of pressure variation on current density in tubular circular FC

G. Graphs With Respect to Tubular Square Model

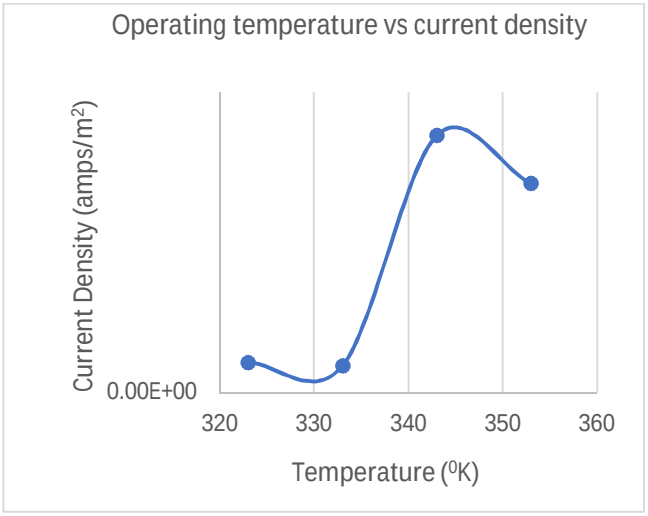

Fig. 25. Effect of temperature variation on current density in tubular square FC

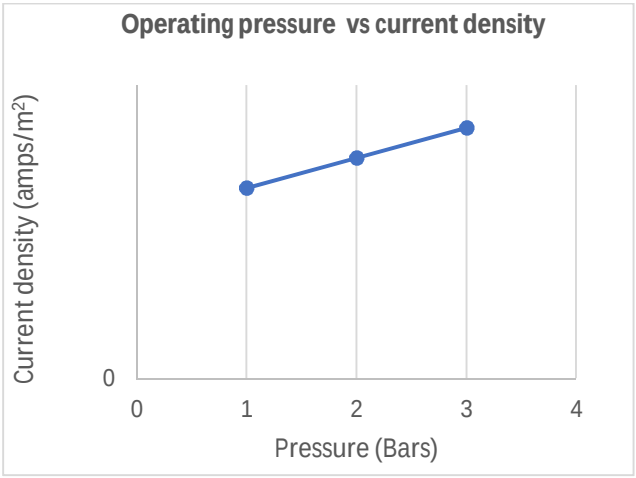

Fig. 26. Effect of pressure variation on current density in tubular square FC

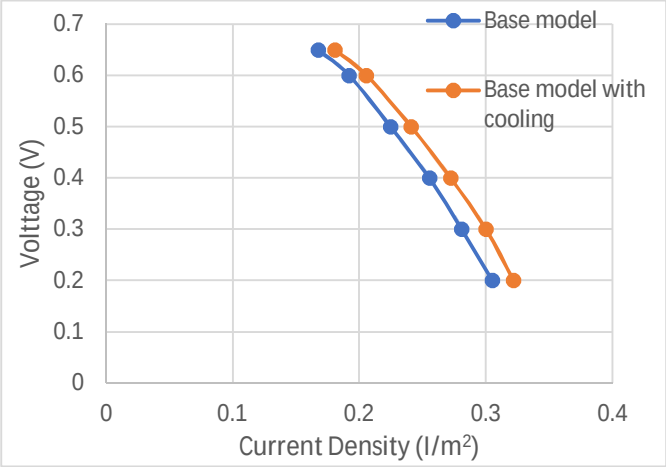

Fig. 27. Polarization graphs of base model with and without cooling

ISSN: 2321-9653; IC Value: 45.98; SJ Impact Factor: 7.538
Volume 10 Issue I Jan 2022- Available at www.ijraset.com

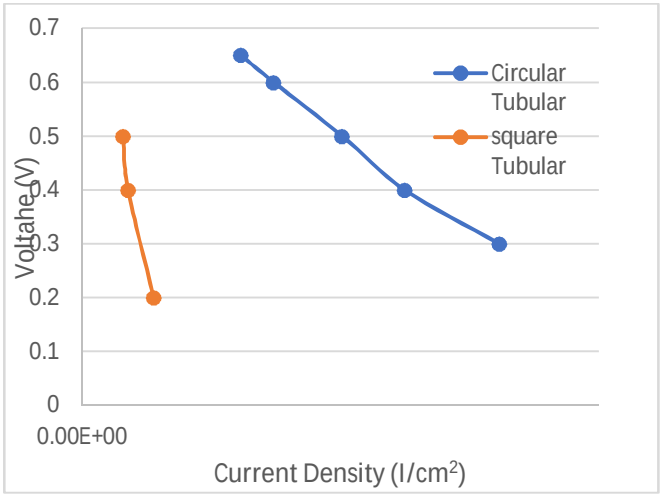

Fig. 28. Polarization graphs of tubular FC models

Maximum temperature vs output voltage in the PEM fuel cell has been plotted at different cooling inlet temperatures. İt can be seen that increase in the voltage upto 0.7V will results in sudden drop of temperature.

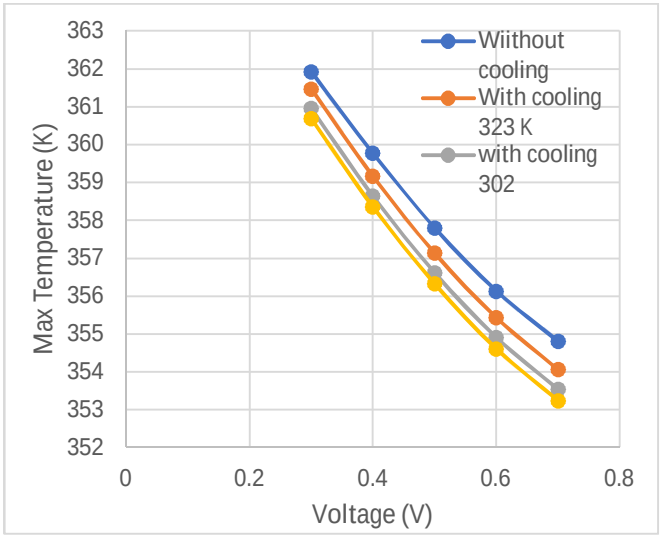

Fig. 29. Effect of cooling temperature on voltage and maximum temperature

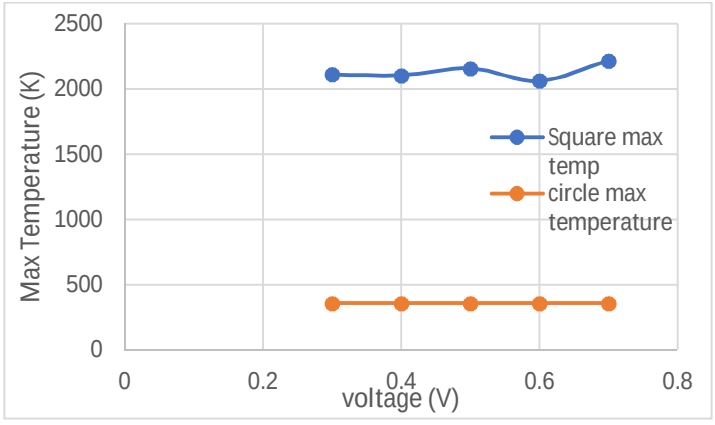

Fig. 30. Variation of max temperature with voltage

H. Max Temperature Graphs

1) W.r.t to H2 species

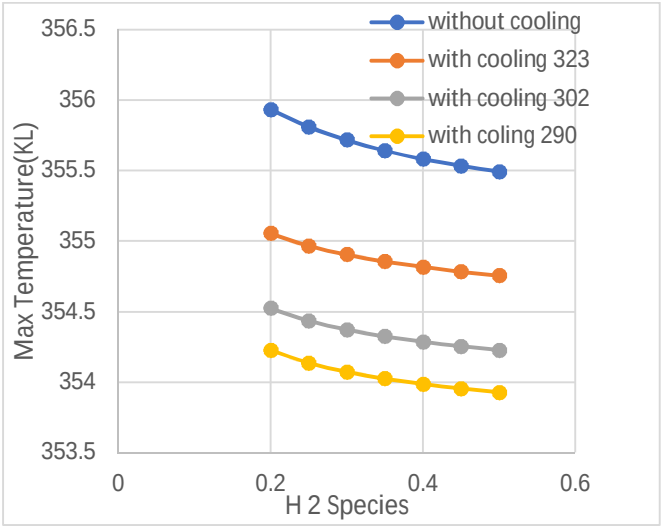

Fig. 31. Effect of cooling temperature with respect to max temp and H2 species

2) Validation

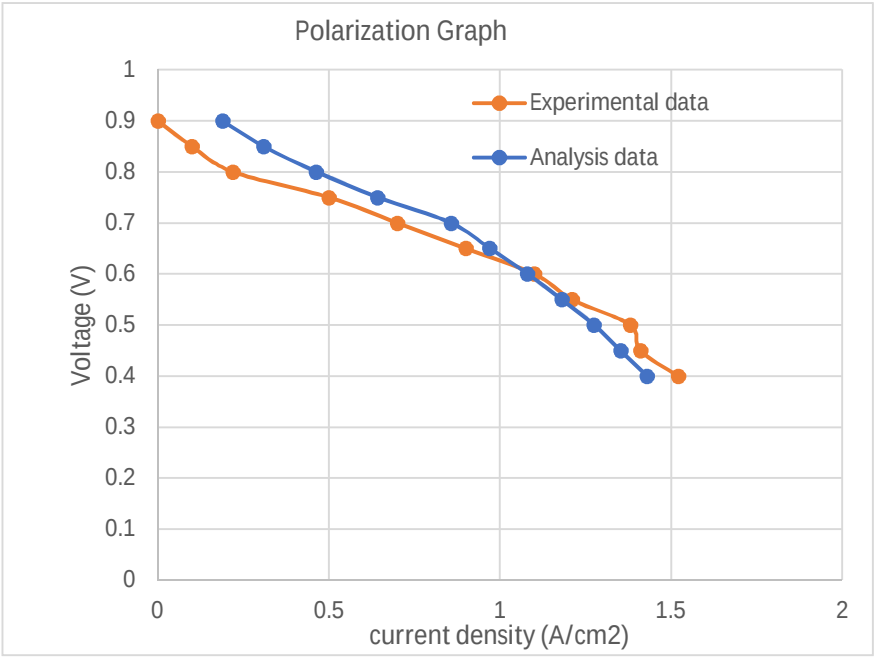

Fig. 33. Model validation

VIII. CONCLUSION

Simulation of single straight channel, PEM fuel cell is carried out with and without liquid cooling system. Under liquid cooling system maximum temperature in the membrane of fuel cell is dropped by 70K if coolant inlet temperature is 290 0K to prevent fuel cell from excessive temperature. Fuel cell temperature distribution is not uniform at anode and cathode. Maximum temperature in cathode channel is greater than maximum temperature at anode channel. With the increase in output voltage up to 0.7V maximum temperature in fuel cell drop suddenly. operating voltage above 0.7V is best to prevent excessive temperature. With increase in the H2 concentration at anode channel decreases the temperature in fuel cell. Hydrogen fraction in anode channel above 0.3 is best to prevent excessive temperature. Comparing polarity curves of Base model PEM Fuel cell with and without cooling, With cooling Configuration shows a good values of current density than base model without cooling.

Comparing the polarity curves indicated that circular tubular configurations propose higher current density compared to the square tubular configurations PEM fuel cell model. But the triangular tubular configuration shows a drop in current density, especially in the low voltages, in comparison with the base PEM fuel cell model and it has not converged to final values as well as iteration during the analysis. Counters of Mass fractions of species on base model shows uniform increase in fraction from gas diffusion layer to gas channel. Vectors of current density in both base model with and without cooling gives uniform formation of vector filed around current collector. Circular tubular architecture indicated more uniform distribution for oxygen and hydrogen mass fraction contours in comparison with the two other architectures and especially with the triangular tubular architecture. Triangular architecture due to its low angle corners prevented uniform reaction so that the range of values in the catalyst and gas diffusion layers was wider. The maximum values existed on the corners, and the species values decreases, and distribution becomes more uniform the further you moved from the corners Due to sharp angle small amount of water content was predicted in the corners of this architecture indicating the slowness of the reaction in these regions. Unlike that case, the circular figure demonstrated a uniform distribution of the exit water vapor due to the uniform distribution of the species. Square architecture power production is placed between the circular and triangular architectures. Temperature distribution contours in gas diffusion and the catalyst layers at the cathode indicated that rising temperature is concentrated away from of the corner regions of the square and triangular architectures due to their sharp angles and slowness of reaction. In the Circular architecture, due to the dispersion of reaction at all surfaces, distribution of rising temperature occurred in wider surfaces and therefore the maximum temperature for this architecture is low. But triangular geometry, due to its non-uniform reaction has the maximum temperature compared with the two other architectures. This damages the catalyst and diffusion layers which results in an undesirable increase in cost especially for the catalyst layer. So, this point should be considered when designing novel high temperature

REFERENCES

[1] C.Y. Wen, G.W. Huang, Application of a thermally conductive pyrolytic graphite sheet to thermal management of a PEM fuel cell, J. Power Sources 178 (1) (2008) 132–140.
[2] C.Y. Wen, Y.S. Lin, C.H. Lu, Performance of a proton exchange membrane fuel cell stack with thermally conductive pyrolytic graphite sheets for thermal management, J. Power Sources 189 (2) (2009) 1100–1105
[3] M.V. Oro, E. Bazzo, Flat heat pipes for potential application in fuel cell cooling, Appl. Therm. Eng. 90 (2015) 848–857.
[4] J. Zhao, Q. Jian, Z. Huang, Experimental study on heat transfer performance of vapor chambers with potential applications in thermal management of proton exchange membrane fuel cells, Appl. Therm. Eng. 180 (2020) 115847
[5] M. Matian, A. Marquis, N. Brandon, Model based design and test of cooling plates for an air-cooled polymer electrolyte fuel cell stack, Int. J. Hydrogen Energy 36 (10) (2011) 6051–6066.
[6] S.M. Baek, S.H. Yu, J.H. Nam, C.J. Kim, A numerical study on uniform cooling of large-scale PEMFCs with different coolant flow field designs, Appl. Therm. Eng. 31 (89) (2011) 1427–1434.
[7] E. Afshari, M. Ziaei-Rad, M.M. Dehkordi, Numerical investigation on a novel zigzag-shaped flow channel design for cooling plates of PEM fuel cells, J. Energy Inst. 90 (5) (2017) 752–763
[8] M.R. Islam, B. Shabani, G. Rosengarten, Nanofluids to improve the performance of PEM fuel cell cooling systems: a theoretical approach, Appl. Energy 178 (2016) 660–671
[9] I.A. Zakaria, W.A.N.W. Mohamed, M.B. Zailan, W.H. Azmi, Experimental analysis of SiO2-distilled water nanofluids in a polymer electrolyte membrane fuel cell parallel channel cooling plate, Int. J. Hydrogen Energy 44 (47) (2019) 25850– 25862.
[10] Odne Burheim, Signe Kjelstrup∗, J.G. Pharoah, Preben J.S. Vie, Steffen Moller-Holst. Calculation of reversible electrode heats in the proton exchange membrane fuel cell from calorimetric measurements.
[11] Jean-Paul Kone1, Xinyu Zhang2, Yuying Yan3, Guilin Hu4 and Goodarz Ahmadi Three-dimensional multiphase flow computational fluid dynamics models for proton exchange membrane fuel cell: A theoretical development.
[12] Maher A.R. Sadiq Al-Baghdadi, A CFD study of hygro–thermal stresses distribution in PEM fuel cell during regular cell operation.

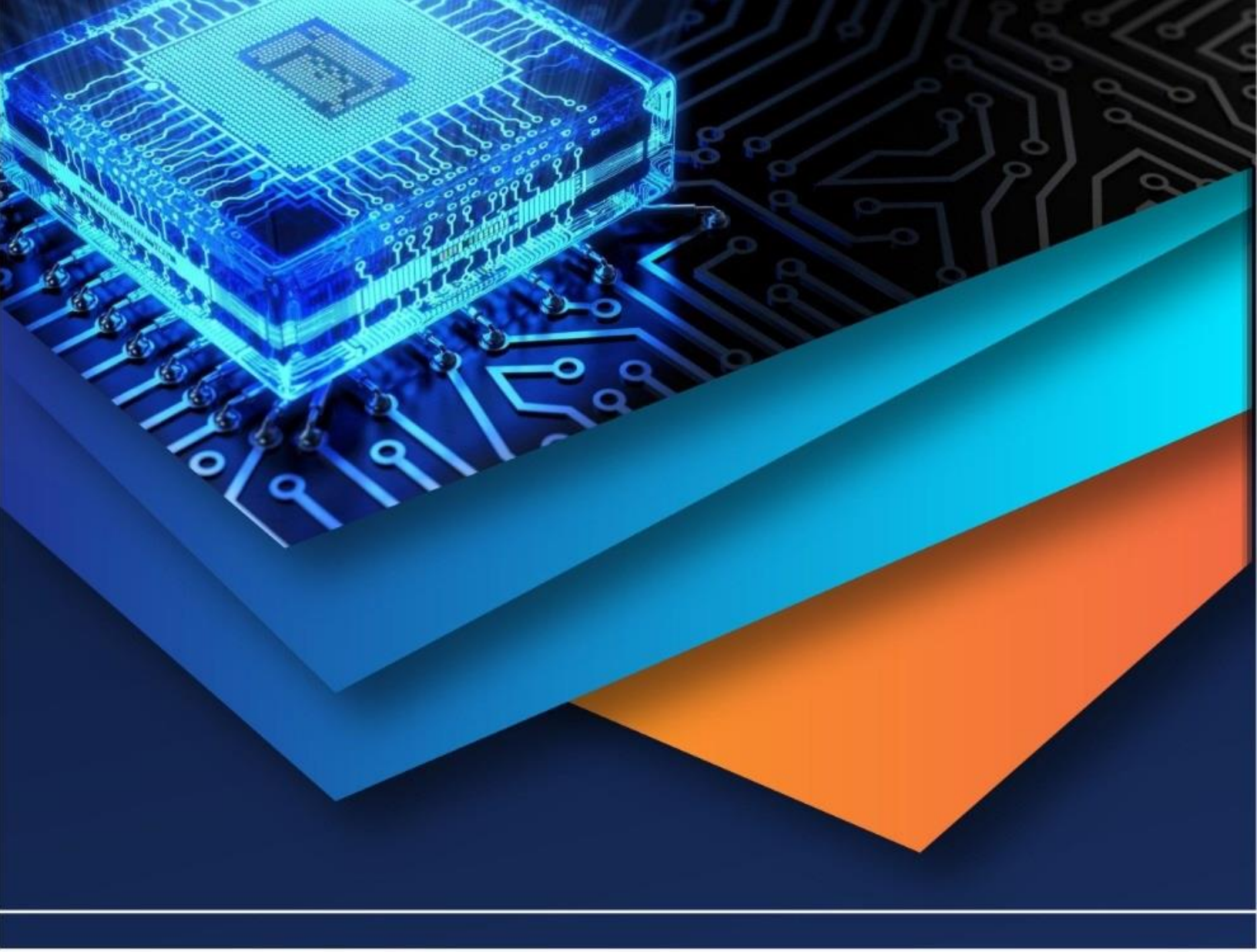

10.22214/IJRASET

45.98

IMPACT FACTOR: 7.129

IMPACT FACTOR: 7.429

INTERNATIONAL JOURNAL FOR RESEARCH

IN APPLIED SCIENCE & ENGINEERING TECHNOLOGY